ADVANCING EARTH AND SPACE SCIENCES

Geophysical Research Letters

RESEARCH LETTER
10.1029/2024GL111814

Deciphering a Quantitative Relationship Between Rifting and Crustal Melt Fraction: Insights From the Incipient Okavango Rift Zone

Tuo Wang[1], **Ling Chen**[1,2], **Stephen S. Gao**[3], and **Kelly H. Liu**[3]

[1]State Key Laboratory of Lithospheric and Environmental Coevolution, Institute of Geology and Geophysics, Chinese Academy of Sciences, Beijing, China, [2]College of Earth and Planetary Sciences, University of Chinese Academy of Sciences, Beijing, China, [3]Department of Earth Sciences and Engineering, Missouri University of Science and Technology, Rolla, MO, USA

Key Points:

- The study reveals a quantitative relationship between crustal extension and crustal melt fraction through a comparative analysis
- For the world's major rifts, the crustal Vp/Vs ratio (κ) is related to the stretching factor (β) by the equation $\kappa = 1.43 + 0.34\beta$
- Melts would be introduced in a rifted crust if the magnitude of stretching is comparable to that of the Okavango Rift Zone

Supporting Information:

Supporting Information may be found in the online version of this article.

Correspondence to:

L. Chen,
lchen@mail.iggcas.ac.cn

Citation:

Wang, T., Chen, L., Gao, S. S., & Liu, K. H. (2025). Deciphering a quantitative relationship between rifting and crustal melt fraction: Insights from the incipient Okavango Rift Zone. *Geophysical Research Letters*, *52*, e2024GL111814. https://doi.org/10.1029/2024GL111814

Received 12 AUG 2024
Accepted 8 JUN 2025

Author Contributions:

Conceptualization: Tuo Wang
Data curation: Kelly H. Liu
Formal analysis: Tuo Wang
Funding acquisition: Tuo Wang
Investigation: Tuo Wang
Methodology: Tuo Wang, Stephen S. Gao
Supervision: Ling Chen
Validation: Ling Chen
Writing – original draft: Tuo Wang
Writing – review & editing: Ling Chen, Stephen S. Gao, Kelly H. Liu

Abstract

Rifting and magmatism are fundamental geological processes in the evolution of the lithosphere; however, quantitative investigations of their relationship are rare. The Okavango Rift Zone (ORZ) is in the early stages of rifting and magmatic activity and thus is an ideal locale to study this relationship. We examine the relationship using two primary crustal structure parameters: crustal thickness and average Vp/Vs ratio obtained from receiver functions. Our large Vp/Vs estimates indicate the existence of melts within the crust of the ORZ. Comparing our results with those of other continental rifts, we identify a quantitative relationship between rifting and crustal melt fraction. Additionally, the comparative analysis suggests that melts within a rift crust are introduced only when the stretching magnitude reaches that of the ORZ. We also propose a model suggesting that with the progression of rifting, melts would be introduced into the crust and increased gradually, potentially triggering rift-related volcanism.

Plain Language Summary

Understanding how rifting and magmatism shape the Earth is crucial for unraveling our planet's evolution. Key question about how rifting and magmstism correlate remains. The young Okavango Rift Zone (ORZ) within the East African Rift System has just started the rifting and magmatic activity, offering a prime opportunity to study these processes. To explore the relationship between rifting and crustal melt fraction, we use receiver functions to measure the crustal thickness and average Vp/Vs ratio within the ORZ and nearby regions. Our findings show the ORZ has a thinner crust relative to the surrounding areas and large crustal Vp/Vs values, indicating the presence of melts within the crust that originated from either the crust or the underlying mantle. Comparing these values with those of other rift zones globally, we observe that crustal Vp/Vs values rise as crustal thickness values fall, suggesting a link between crustal thinning and melt fraction. This relationship is further supported by a quantitative analysis, highlighting that a certain extent of crustal extension is necessary to introduce melts into the rift crust. Our model proposes three stages of rift evolution: initial stretching without any magmatic activity, sufficient stretching introducing melts, and further rifting potentially leading to volcanism.

1. Introduction

Rifting and magmatic activity play critical roles in the evolution of the Earth by shaping the surface, creating new continents, and permanently modifying the structure and composition of the Earth's interior. The presence of melts is commonly inferred from geophysical and geochemical studies beneath continental rifts, either in the crust or underlying mantle (e.g., Furman, 2007; Hodgson et al., 2017; Keranen et al., 2004; Mayle & Harry, 2023; Rooney, 2020; Wright et al., 2006). Several factors could account for the generation of melts, such as the presence of volatiles (e.g., water and carbon dioxide) (Dasgupta & Hirschmann, 2006; Foley et al., 2009) and the elevated temperature or reduced pressure due to the lithospheric stretching (e.g., Rychert et al., 2012; R. S. White et al., 2008). It is widely accepted that an inherent relationship exists between rifting and magmatism, though its exact characteristics remain substantially ambiguous. Several key questions persist, contributing to this uncertainty. For instance, why are only certain continental rifts associated with magmatism, and why does the degree of magmatic activity vary among them? Might there be a quantitative correlation between these two fundamental geological processes? These queries underscore the complexity of the interplay between rifting and magmatism, emphasizing the need for further investigation to decode this relationship.

10.1029/2024GL111814

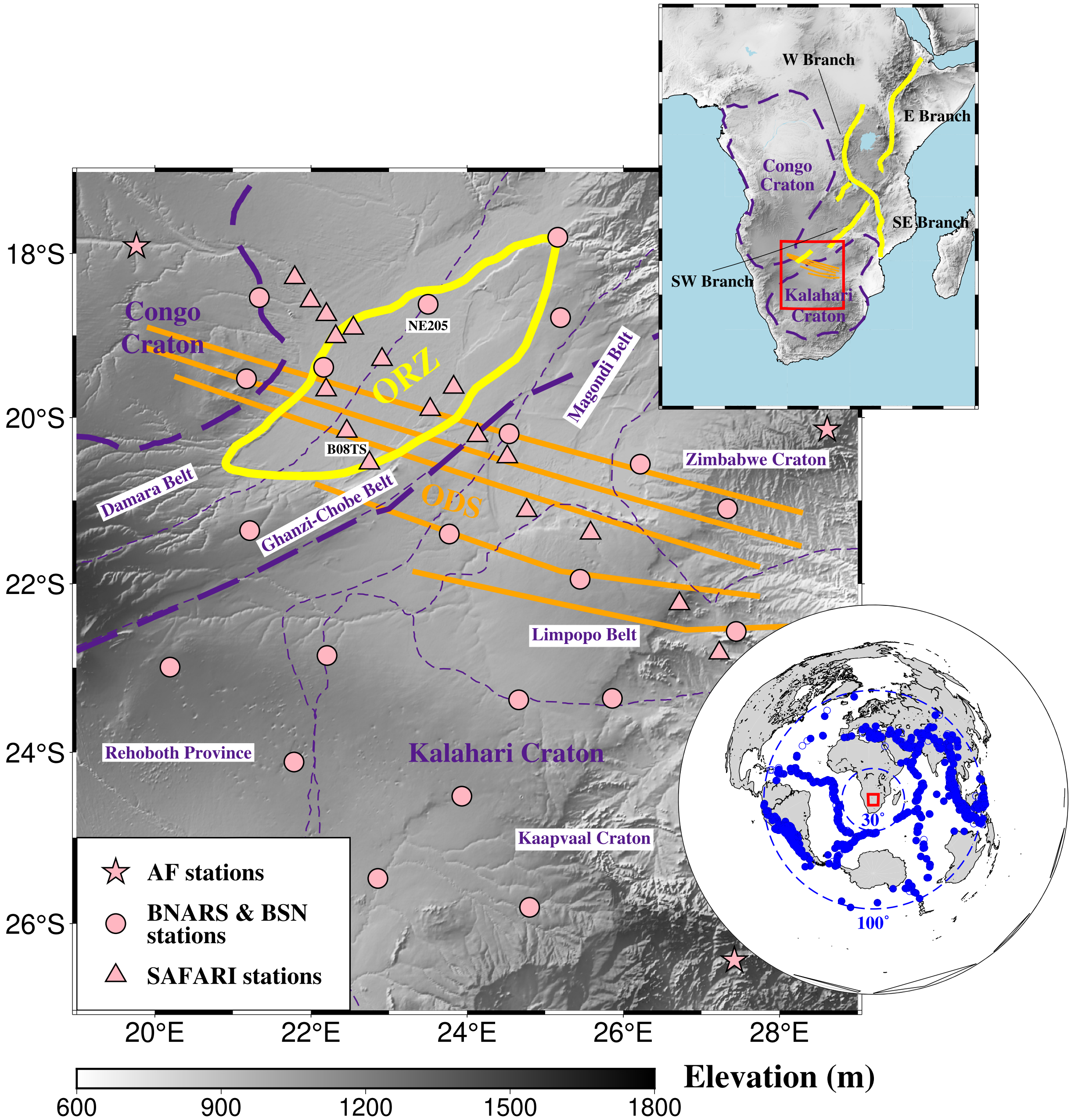

Figure 1. Topographic map of the study region showing the seismic stations (pink symbols). The thick yellow curve encloses the Okavango Rift Zone, and the thick orange curves represent the Okavango Dyke Swarm. The thin violet dashed curves separate the major tectonic units of the study region, and the thick violet dashed curves are the boundaries of the Congo and Kalahari cratons. The inset in the upper right corner shows the location of the study region (red open rectangle) in Africa, with the East African Rift System denoted as yellow curves. The inset in the lower right corner shows the distribution of the teleseismic events requested (blue open circles) and used (blue solid circles) plotted on an azimuthal equidistant projection map. The two big blue dashed circles represent the epicentral distance of 30° and 100°, respectively.

The incipient Okavango Rift Zone (ORZ) (~120-40 Ka, Moore & Larkin, 2001; Reeves, 1972) of the Cenozoic East African Rift System (EARS) (~45 Ma, Boone et al., 2019; Ebinger & Sleep, 1998; George et al., 1998) may reveal how the magmatic activity is involved during the early-stage rifting, and thus it is an ideal locale to decipher the relationship. The ORZ develops between the Neoproterozoic-early Paleozoic Damara Belt to its northwest and the Mesoproterozoic-Neoproterozoic Ghanzi-Chobe Belt to its southeast (Figure 1), with an extension rate of ~0.4 mm/yr (Wedmore et al., 2021). It has been suggested that the Damara-Ghanzi-Chobe Belt is a pre-existing mechanically weak zone developed by the Neoproterozoic collision between the Congo Craton and the composite Kalahari Craton (Begg et al., 2009) which mainly composes of the Zimbabwe and Kaapvaal cratons with the Limpopo Belt caught in between.

Although the rifting of the EARS could be associated with mantle plumes (Hansen et al., 2012; Nyblade & Robinson, 1994; Tsekhmistrenko et al., 2021) since the rift system is developing above the African Large Low Shear Velocity Province (Lithgow-Bertelloni & Silver, 1998; Ni et al., 1999; Ritsema et al., 1998), the initiation of the ORZ is proposed to be induced by intra-plate movements between the Congo and Kalahari cratons (Yu, Gao, et al., 2015). Beneath the ORZ, a localized low-velocity anomaly constrained in the upper mantle is revealed by previous tomography studies (Fadel et al., 2020; Ortiz et al., 2019). The low-velocity anomaly is interpreted as partial melts induced by lithospheric stretching (Fadel et al., 2020). The melts assist in weakening the lithosphere and localizing strain, providing a more suitable condition for the rift initiation (Leseane et al., 2015).

In the present study, we apply the receiver function (RF) H-κ stacking analysis (Zhu & Kanamori, 2000) to estimate the crustal thickness (H) and crustal average Vp/Vs ratio (κ) beneath the ORZ and adjacent regions. A resonance removal technique (Yu, Song, et al., 2015) is applied to suppress the reverberations on RFs caused by the unconsolidated sediments. The thickness of the crust provides insights into the stretching/rifting magnitude of the continental crust. The Vp/Vs ratio increases exponentially with a linear increment in fluid percentage, since Versus decreases faster than Vp, and thus it could indicate the crustal melt fraction (Watanabe, 1993). We first discuss the presence of melts within the crust of the ORZ. Subsequently, we make a series of comparisons between the ORZ and other continental rift zones globally to investigate the quantitative relationship between the continental stretching/rifting and crustal melt fraction.

2. Data and Methods

The present study gathered available seismic data from 62 broadband seismic stations within the study region (Figure 1). The stations include 3 permanent stations of the AfricaArray (AF), 21 stations of the Botswana Network of Autonomously Recording Seismographys (BNARS), 21 stations of the Botswana Seismological Network (BSN), and 17 stations of the Seismic Arrays for African Rift Initiation experiment. Considering the BNARS and BSN experiments share the same 21 station sites, we labeled the sites using the names of the stations with more data. Data recorded at a same station site were combined and processed together.

The three-component broadband seismograms used are from teleseismic events within the epicentral distance range of 30°–100° (inset in the lower right corner of Figure 1). The seismograms were then preprocessed (details can be found in Text S1 in Supporting Information S1), and radial RFs were calculated from the preprocessed seismograms based on a frequency-domain water-level deconvolution (Ammon, 1991; Clayton & Wiggins, 1976). Considering the presence of unconsolidated sediments as thick as ~2.5 km in the ORZ (Pretorius, 1984; Ringrose et al., 2005), an autocorrelation frequency-domain resonance removal filter (Yu, Song, et al., 2015) was applied to suppress the near-surface reverberations on the resulting RFs caused by the strong impedance between the upper crust and low-velocity sedimentary layers (Figure S1 in Supporting Information S1). We then followed the conventional H-κ stacking procedure (Zhu & Kanamori, 2000) to grid-search for the optimal combination of H and κ estimates at each of the station sites. To check the reliability of the H and κ estimates, a bootstrap method was applied for obtaining the mean and standard deviation values (Efron & Tibshirani, 1986) (Text S1 in Supporting Information S1).

3. Results

In total, 33 station sites yield reliable H and κ estimates, and the spatial distributions and uncertainty estimates are shown in Figure 2. The mean H value of the study region is ~41.5 ± 3.2 km with the thinnest crust found at Station NE215 (~35.8 km), located near the northeastern tip of the ORZ, and the thickest crust found at Station NE218 (~47.5 km), located in the westernmost portion of the Zimbabwe Craton (Figure 2a). The mean κ value of the region is ~1.77 ± 0.04, a value that is quite close to the global average value of 1.78 (Christensen, 1996). The largest κ value of ~1.91 was estimated at Station B06OR in the central portion of the ORZ, while the smallest value of ~1.68 was found at Station WDLM in the Kaapvaal Craton (Figure 2b). The STDs for the H and κ estimates are lower than 0.5 km and 0.02 (Figures 2c and 2d), respectively, suggesting an overall high reliability for the study area.

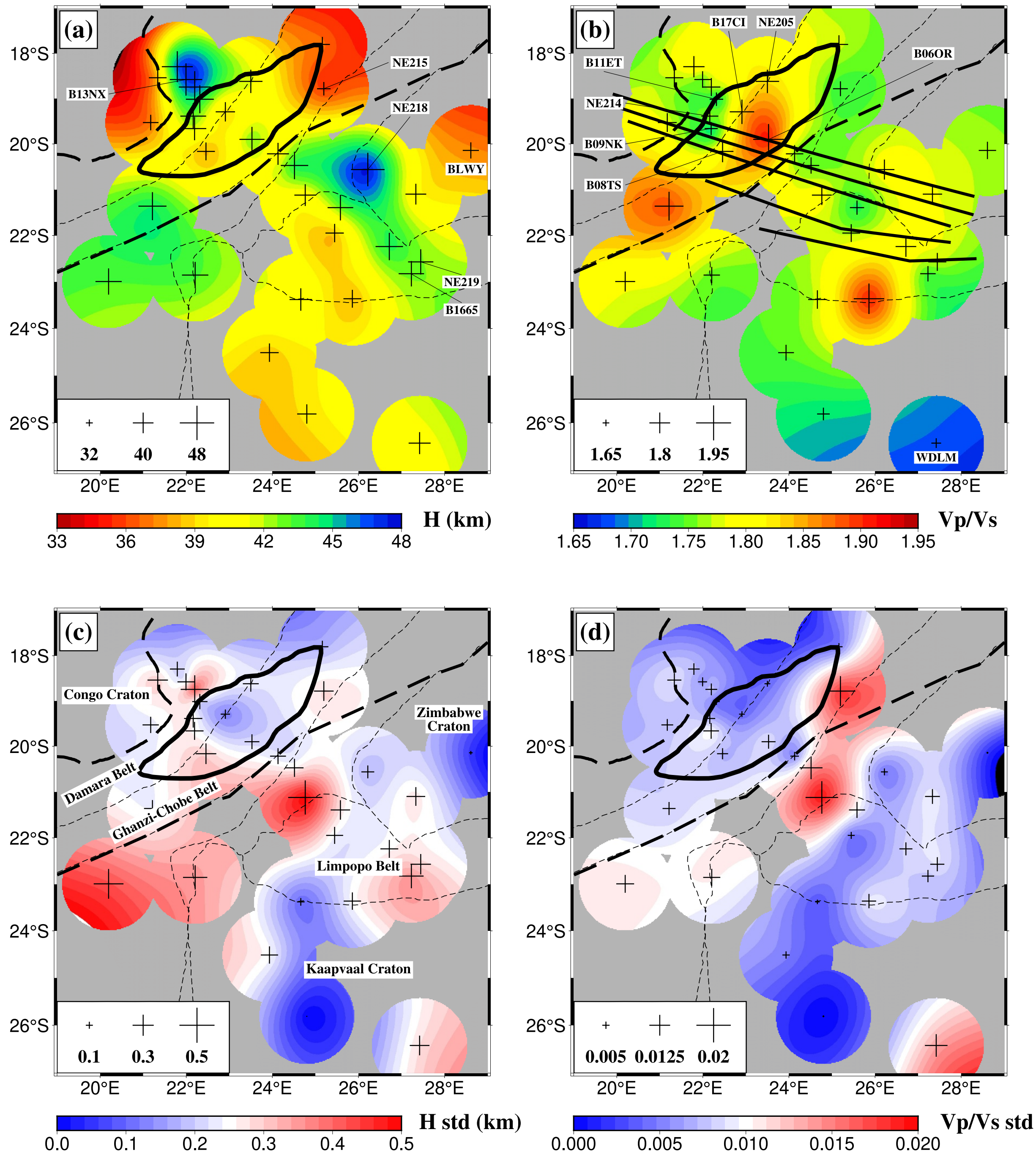

Figure 2. (a) Map of crustal thickness (H). (b) Map of crustal average Vp/Vs ratio (κ). (c) Standard deviation (STD) of H estimates from bootstrapping. (d) STD of κ estimates from bootstrapping. The cross symbols represent individual estimates.

Comparing with the surrounding regions, the ORZ is characterized by relatively thinner crust and larger κ values. For the 7 stations located within the rift valley (stations B06OR, B08TS, B09NK, B11ET, B17CI, NE205, and NE214; Figure 2b), the average H and κ values are ~41.5 ± 2.1 km and 1.80 ± 0.07. Small H and large κ values concentrate along the rift axis. The average H and κ values become ~40.0 ± 2.2 km and 1.85 ± 0.05 if excluding the four stations located near the rift shoulders (stations B09NK, B11ET, NE205, and NE214). Outside the ORZ, small H estimates are mainly found in the northeastern portion of the Damara-Ghanzi-Chobe Belt, Congo Craton, Kaapvaal Craton, and the Zimbabwe Craton with the exception of its southwestern portion. Large κ estimates are observed in the southwestern portion of the Damara-Ghanzi-Chobe Belt and the Limpopo Belt. The observations are generally consistent with those from previous RF studies (Fadel et al., 2018; Yu, Liu, et al., 2015). Quantitative comparisons among these studies further support the consistency and the reliability of our estimates (Text S2 in Supporting Information S1).

4. Discussion

The presence of complex crustal structures, such as dipping layers and anisotropy, could lead to azimuthal variations of the H and κ estimates (Cassidy, 1992; Levin & Park, 1997; Link et al., 2020; Lombardi et al., 2008). To analyze the potential effects of such structures, we performed a series of tests at the two stations with large κ estimates (>1.85) within the ORZ (Figures S4 and S5, Text S3 in Supporting Information S1). We divided the RFs into four groups, based on the back azimuths, that is, 0–90°, 90–180°, 180–270°, and 270–360°. Due to the uneven distribution of global seismicity, most events are from the first and third quadrants. Our tests show that for the two stations, the H and κ estimates using events from the two quadrants are statistically consistent with each other and with the estimates when all the events are used. This consistency indicates that possible complex crustal structures do not have a significant effect on the results.

4.1. Melts Within the Rift's Crust

The large κ estimates in the ORZ (Figure 2) may be attributed to the composition variation. Usually, κ values increase with the proportion of mafic or ultramafic rocks in the crust (Christensen, 1996). Mafic or ultramafic rocks are possibly solidified from intruded mantle magmas, as observed underneath the Baikal Rift Zone (Thybo & Nielsen, 2009), Afar Depression (Hammond et al., 2011), and the Main Ethiopian Rift Zone of the EARS (Dugda et al., 2005). In our study area, the magmatic intrusion could be associated with the Okavango Dyke Swarm at ca. ~179 Ma (Le Gall et al., 2002) cutting through the central ORZ, where large κ estimates were observed (Figure 2b). However, the experimental κ value for solid basalt in the crust ranges from ~1.84 to 1.86 (Christensen, 1996), suggesting that our large κ estimates up to ~1.91 may not be solely caused by the mafic composition of ancient intrusions. Although the intrusions may result in underplating at the Moho and thus introduce uncertainties to our κ estimates (Ogden et al., 2019), the significant P-to-S conversions from the Moho (Pms) of the stacked RFs from all stations show little sign of underplating.

Alternatively, melts in the crust could play a critical role in elevating κ values. Based on experiment results, κ values greater than 1.82 can be attributed to the increment of crustal melt fraction (Watanabe, 1993), assuming other effects such as from the temperature or melt geometry are excluded (Clemens & Vielzeuf, 1987; Takei, 2002). The large κ estimates found around the rift axis (~1.85, Figure 2b) may suggest the presence of crustal melts. A recent study shows that a κ value of 1.90 corresponds to ~10% melt volume (Feng et al., 2023).

The melts could be generated by decompression melting in the upper mantle due to the stretching of the lithosphere (Acocella, 2014; Keen et al., 1994) and subsequently intrude into the crust. The current lithospheric thickness of the ORZ could reach as low as ~130 km (Afonso et al., 2022). Given that the ORZ developed in the Damara-Ghanzi-Chobe Belt, we assume the lithospheric thickness of the belt (~220 km, Afonso et al., 2022) as the prerift thickness. The lithospheric stretching factor, the ratio between current and prerift thickness of the lithosphere, is thus ~1.69 beneath the ORZ, which is large enough to induce decompression melting (R. White & McKenzie, 1989). Although the estimated stretching factor might be affected by uncertainties in reconstructing the prerift lithospheric thickness, the presence of the decompression-induced melts is further supported by a previously revealed low-velocity anomaly in the upper mantle (Fadel et al., 2020; Ortiz et al., 2019).

The melts could be also generated through crustal partial melting associated with high temperatures. The heat flow of ~70.0 $\mathrm{mW/m^2}$ within the ORZ (Leseane et al., 2015) is just slightly higher than the average heat flow of ~64.7 $\mathrm{mW/m^2}$ for global continents (Davis, 2013), which is apparently insufficient to induce crustal partial melting. Magmatic intrusion from the mantle could heat the lower or even the middle crust and may subsequently induce crustal partial melting.

4.2. Quantitative Relationship Between Rifting and Crustal Melt Fraction

To discern the quantitative correlation between rifting and crustal melt fraction, we undertook a comparative analysis across major continental rifts globally (Figure 3). We first compared the average H and κ values calculated from each investigation (H_{ave} and κ_{ave}) of the ORZ with those of other major EARS rift zones

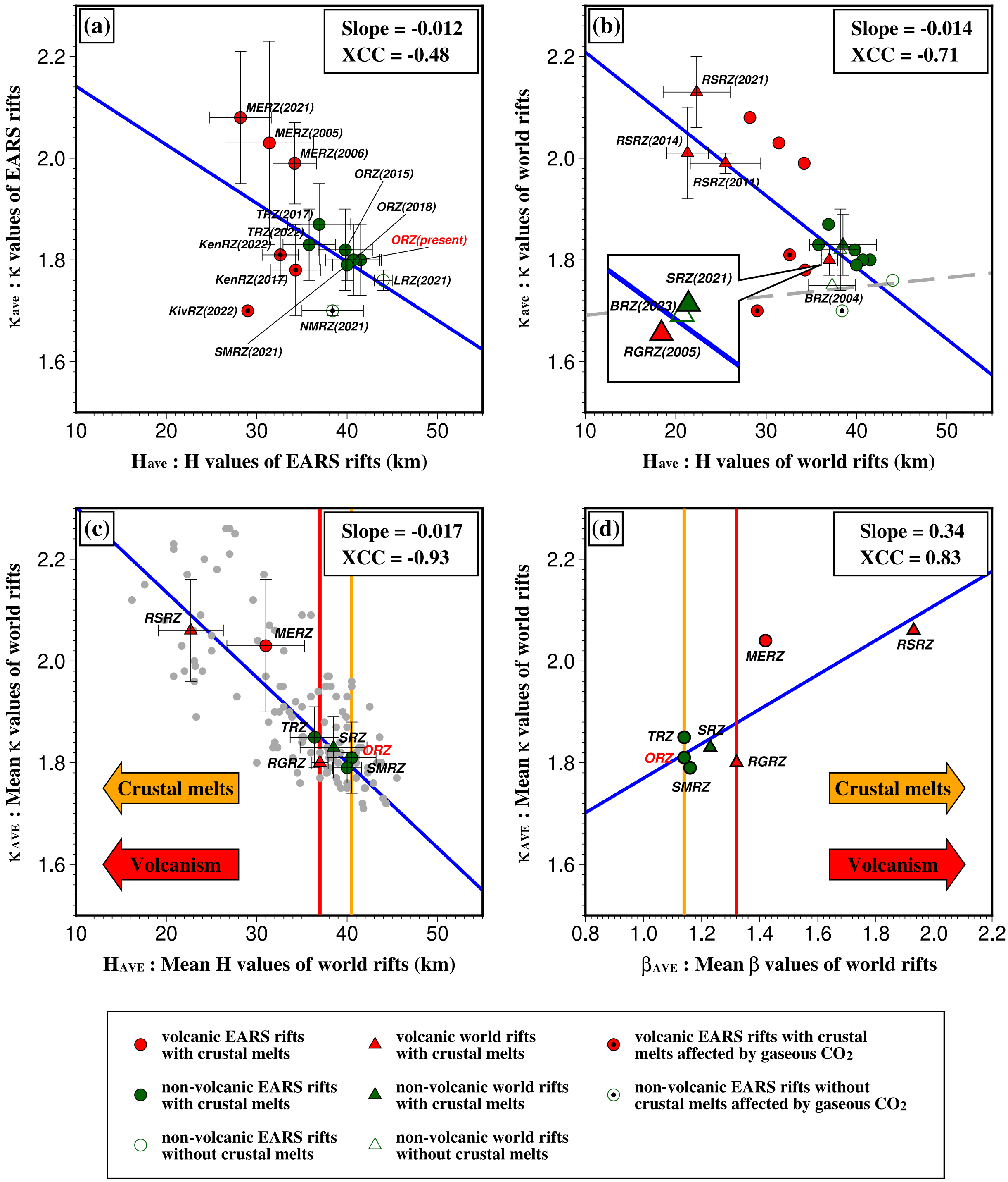

Figure 3. Comparisons of H-κ (a–c) and β-κ pairs (d) among different rift zones. (a) Comparison among East African Rift System (EARS) rift zones (circles) from different investigations. The H_{ave} and κ_{ave} represent the average values calculated from each investigation. (b) Similar to (a), but for comparison among global rift zones by adding four additional ones outside the EARS (triangles). (c) Comparison among global rift zones by averaging the H_{ave} and κ_{ave} values (H_{AVE} and κ_{AVE}). The small gray dots represent individual estimates from different investigations. (d) Similar to (c), but for β_{AVE} and κ_{AVE} comparison among global rift zones. Details for obtaining the H_{ave}, κ_{ave}, H_{AVE}, κ_{AVE}, and β_{AVE} values can be found in Text S4 in Supporting Information S1. Abbreviations of rift zones: BRZ: Baikal; KenRZ: Kenya; KivRZ: Kivu; LRZ: Luangwa; MERZ: Main Ethiopian; NMRZ: northern Malawi; ORZ: Okavango; RGRZ: Rio Grande; RSRZ: Red Sea; SMRZ: southern Malawi; SRZ: Shanxi; TRZ: Tanganyika. Abbreviations with year numbers represent the source of the data used for comparisons, for example, MERZ(2021) in (a) represents data from Wang et al. (2021). XCC: cross-correlation coefficient.

(Figure 3a). The H and κ values can vary dramatically from rift valleys to shoulders (Hopper et al., 2020), and to focus on the stretching, we only considered values within the rift valleys for calculating the H_{ave} and κ_{ave} (Text S4 and Table S1 in Supporting Information S1). A negative correlation (blue line in Figure 3a), with the absolute slope and cross-correlation coefficient (XCC) values of 0.012 and 0.48, respectively, indicates that the κ_{ave} values elevate with the decrease of H_{ave} values. Melts have been suggested within the crust beneath most of the EARS rift zones (solid circles in Figure 3a) (Chorowicz, 2005; Ebinger & Casey, 2001; Fadel et al., 2018; Hodgson et al., 2017; Plasman et al., 2017; Roecker et al., 2017; Sun et al., 2021; Wang et al., 2021, 2022; WoldeGabriel et al., 1990) with the only two exceptions of the Luangwa Rift Zone and the northern Malawi Rift Zone of the magma-poor Western Branch of the EARS (open circles in Figure 3a). Therefore, the negative correlation supports the general recognition that the crustal melt fraction, as represented by κ values, increases with the extent of crustal thinning/rifting.

To validate the correlation, we included four narrow Cenozoic continental rift zones elsewhere in our examination (triangles in Figure 3b), the Red Sea Rift Zone to the north of the EARS, Rio Grande Rift Zone in southwestern United States, Shanxi Rift Zone in the central North China Craton, and the Baikal Rift Zone in central Eurasia (Figure S7 in Supporting Information S1). Rift-introduced melts have been suggested within the crust of the first three of these rift zones (solid triangles in Figure 3b) (Cipar et al., 2020; Reed et al., 2014; H. Xu et al., 2020; X. Xu & Ma, 1992). Although the Baikal Rift Zone is one of the most seismically active rifts on Earth, no melts have been proposed in the rift crust (open triangles in Figure 3b). The negative correlation still holds after adding these global rift zones, and the absolute slope value of the correlation (0.014) is comparable with that for the EARS rift zones (0.012), further verifying the relationship.

However, the absolute value of XCC becomes greater (from 0.48 to 0.71), suggesting a stronger connection (Figure 3b). This may be attributed to the presence of gaseous CO_2 in several EARS rift zones (symbols with black bull eyes in the center in Figures 3a and 3b). Rift zones with gaseous CO_2 in the crust are not well-constrained by the negative correlation since the gaseous CO_2 could decrease Vp/Vs values (Plasman et al., 2017; Roecker et al., 2017; Sun et al., 2021) (Text S5 in Supporting Information S1). Additionally, rift zones without melts in the crust (open symbols in Figure 3) are not necessarily constrained by the correlation. For these non-melt and CO_2-affected rift zones, the κ_{ave} is not sensitive to the variation of H_{ave} (gray dashed line in Figure 3b). Considering this, we exclude the non-melt and CO_2-affected rift zones in the future analysis and averaged all the H_{ave} and κ_{ave} values from different investigations of each rift zone, as represented by H_{AVE} and κ_{AVE} (Figure 3c). A more intuitive and rational correlation was obtained with the greater absolute slope and XCC values of 0.017 and 0.93, suggesting a stronger connection between the two crustal parameters.

Besides using the H values, we also compared the crustal stretching factor (β, the ratio of present-day to prerift crustal thickness) with the κ values in the analysis. Figure 3d reveals a positive correlation between the averaged β values from different investigations of each rift zone (β_{AVE}, see details in Text S4 in Supporting Information S1) and κ_{AVE} with a slope of 0.34 and XCC of 0.83. More importantly, we found that the crustal Vp/Vs ratio (κ) and the crustal stretching factor (β) are related by an equation of $\kappa = 1.43 + 0.34\beta$, which quantitatively supports the view that the crustal melt fraction elevates with the increasing extent of crustal extension.

4.3. A Three-Stage Rifting Model

One distinctive feature from the comparative analysis is that the ORZ is characterized by the largest H/smallest β and almost the smallest κ values among all the rift zones with melts in the crust (Figures 3c and 3d). This suggests that for a certain rift zone, if the crust has not been thinned enough, that is $H_{AVE} > 40.5$ km in our study (vertical orange line in Figure 3c), or has not been suffiently stretched, that is $\beta_{AVE} < 1.14$ (vertical orange line in Figure 3d), melts would not be introduced into the rift crust. Therefore, the crustal thickness and crustal stretching factor of the incipient ORZ represent the thresholds for introducing melts into the crust.

Another interesting feature is that rift-related volcanism is mostly found at rift zones characterized by thin crust ($H_{AVE} \leq 37.0$ km, vertical red line in Figure 3c) or well-stretched crust ($\beta_{AVE} \geq 1.32$, vertical red line in Figure 3d), which are the Main Ethiopian Rift Zone (Baker et al., 1996; Ebinger & Casey, 2001), Rio Grande Rift Zone (Grauch et al., 2017), and the Red Sea Rift Zone (Hammond et al., 2011; Wolfenden et al., 2005). For the non-volcanic rift zones (green symbols in Figures 3c and 3d), volcanism would be triggered once the crust reaches a critical threshold of thinning/stretching.

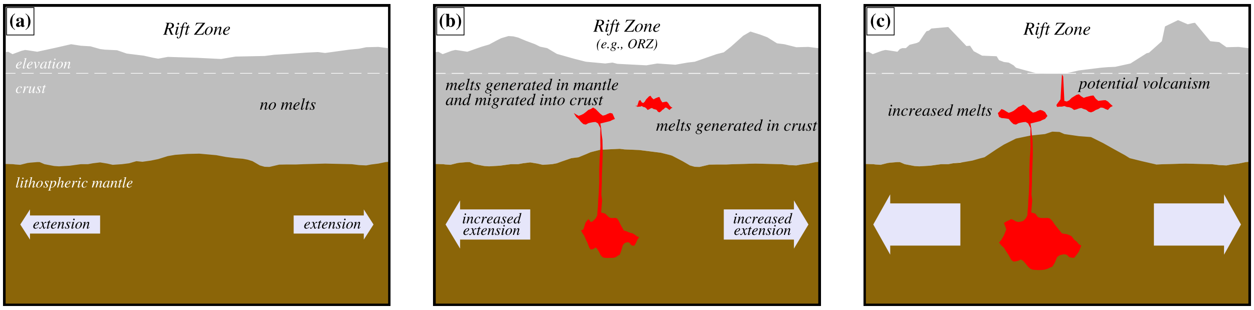

Figure 4. Schematic diagrams showing the relationship between rifting and melting processes beneath a rift zone. (a) The lithosphere of the rift zone has not been sufficiently stretched to introduce melts. (b) Melts are generated when the rifting reaches a certain degree. (c) The amount of melts increases as rifting continues, and rift-related volcanism may be induced as rifting progresses.

We propose a three-stage model of rifting that involves melting and volcanism. In the first stage, the rift crust has not been sufficiently thinned/stretched to introduce melts into the crust (Figure 4a). During the next stage, melts are introduced as the accumulation of crustal extension, whether they are generated in the crust or in the underlying mantle (Figure 4b). The ORZ represents the initiation of this stage. In the last stage, the volume of melts within the crust increases with the progression of rifting, and rift-related volcanism may be triggered as the stretching continues to a critical threshold (Figure 4c).

5. Conclusions

We estimate crustal thickness and crustal average Vp/Vs ratio in the ORZ and adjacent regions using a RF H-κ stacking analysis assisted with a resonance removal technique. Our results indicate that the ORZ is characterized by reduced crustal thickness and elevated crustal Vp/Vs values. The observations are indicative of the combined effects of magmatic intrusions associated with the Okavango Dyke Swarms and the presence of melts in the crust due to continental extension. By comparing the crustal thickness/stretching factor and crustal Vp/Vs values across various continental rift zones within the EARS and other global regions, we reveal a quantitative relationship between rifting and crustal melt fraction. Further analysis on the relationship gives an equation ($\kappa = 1.43 + 0.34\beta$) that relates the crustal Vp/Vs ratio (κ) and crustal stretching factor (β). Additionally, the stretching magnitude of the ORZ, with the crust is thinned to 40.5 km and the crustal stretching factor reaches 1.14, represents a threshold for melts to be introduced into the crust. We propose a model suggesting that melts could be introduced into the crust and increased with the progression of rifting, and rift-related volcanism might be triggered once the rifting reaches a certain extent.

Acknowledgments
We acknowledge the efforts of the staff at the Botswana Geoscience Institute for installing and maintaining the seismic stations. The Seismological Facility for the Advancement of Geosciences Data Management Center (SAGE DMC) was used for access to waveforms and related metadata. SAGE Data Services are funded by the U.S. National Science Foundation (NSF) under Cooperative Support Agreement EAR-1851048. Constructive reviews from two anonymous reviewers and Editor Christian Huber greatly improved the manuscript. This research is funded by the National Natural Science Foundation of China (Grant 42304059) to T.W., and supported by the National Natural Science Foundation of China (Grant 42288201) to L.C., the U.S. NSF under award 1919789 to S.G., and the American Chemical Society Petroleum Research Fund 65563-ND8 to K.L. Figures presented were generated using the Generic Mapping Tools (Wessel et al., 2019).

Data Availability Statement

The seismic data used in the study are archived at the SAGE DMC (https://ds.iris.edu/ds/nodes/dmc). The BREQ_FAST procedure is used for requesting data with detailed information in http://ds.iris.edu/ds/nodes/dmc/forms/breqfast-request (last accessed: September 2022). The seismic stations used are part of the following open networks: (a) the AF (Penn State University, 2004); (b) the BX (Botswana Geoscience Institute, 2001); (c) the NR (Utrecht University, 1983); (d) the XK (Gao et al., 2012).

References

Acocella, V. (2014). Structural control on magmatism along divergent and convergent plate boundaries: Overview, model, problems. *Earth-Science Reviews*, *136*(4), 226–288. https://doi.org/10.1016/j.earscirev.2014.05.006

Afonso, J. C., Ben-Mansour, W., O'Reilly, S. Y., Griffin, W. L., Salajegheh, F., Foley, S., et al. (2022). Thermochemical structure and evolution of cratonic lithosphere in central and southern Africa. *Nature Geoscience*, *15*(5), 405–410. https://doi.org/10.1038/s41561-022-00929-y

Ammon, C. J. (1991). The isolation of receiver effects from teleseismic P waveforms. *Bulletin of the Seismological Society of America*, *81*(6), 2504–2510. https://doi.org/10.1785/bssa0810062504

Baker, J., Snee, L., & Menzies, M. (1996). A brief Oligocene period of flood volcanism in Yemen: Implications for the duration and rate of continental flood volcanism at the Afro-Arabian triple junction. *Earth and Planetary Science Letters*, *138*(1–4), 39–55. https://doi.org/10.1016/0012-821x(95)00229-6

Begg, G. C., Griffin, W. L., Natapov, L. M., O'Reilly, S. Y., Grand, S. P., O'Neill, C. J., et al. (2009). The lithospheric architecture of Africa: Seismic tomography, mantle petrology, and tectonic evolution. *Geosphere*, *5*(1), 23–50. https://doi.org/10.1130/ges00179.1

Boone, S. C., Kohn, B. P., Gleadow, A. J. W., Morley, C. K., Seiler, C., & Foster, D. A. (2019). Birth of the East African Rift System: Nucleation of magmatism and strain in the Turkana depression. *Geology*, *47*(9), 886–890. https://doi.org/10.1130/g46468.1

Botswana Geoscience Institute. (2001). Botswana seismological network [Dataset]. *International Federation of Digital Seismograph Networks*. https://doi.org/10.7914/SN/BX

Cassidy, J. F. (1992). Numerical experiments in broad-band receiver function analysis. *Bulletin of the Seismological Society of America*, *82*(3), 1453–1474. https://doi.org/10.1785/bssa0820031453

Chorowicz, J. (2005). The East African Rift System. *Journal of African Earth Sciences*, *43*(1–3), 379–410. https://doi.org/10.1016/j.jafrearsci.2005.07.019

Christensen, N. I. (1996). Poisson's ratio and crustal seismology. *Journal of Geophysical Research*, *101*(B2), 3139–3156. https://doi.org/10.1029/95jb03446

Cipar, J. H., Garber, J. M., Kylander-Clark, A., & Smye, A. J. (2020). Active crustal differentiation beneath the Rio Grande Rift. *Nature Geoscience*, *13*(11), 758–763. https://doi.org/10.1038/s41561-020-0640-z

Clayton, R. W., & Wiggins, R. A. (1976). Source shape estimation and deconvolution of teleseismic bodywaves. *Geophysical Journal International*, *47*(1), 151–177. https://doi.org/10.1111/j.1365-246x.1976.tb01267.x

Clemens, J. D., & Vielzeuf, D. (1987). Constraints on melting and magma production in the crust. *Earth and Planetary Science Letters*, *86*(2–4), 287–306. https://doi.org/10.1016/0012-821x(87)90227-5

Dasgupta, R., & Hirschmann, M. M. (2006). Melting in the Earth's deep upper mantle caused by carbon dioxide. *Nature*, *440*(7084), 659–662. https://doi.org/10.1038/nature04612

Davis, J. H. (2013). Global map of solid Earth surface heat flow. *Geochemistry, Geophysics, Geosystems*, *14*(10), 4608–4622. https://doi.org/10.1002/ggge.20271

Dugda, M. T., Nyblade, A. A., Julia, J., Langston, C. A., Ammon, C. J., & Simiyu, S. (2005). Crustal structure in Ethiopia and Kenya from receiver function analysis: Implications for rift development in eastern Africa. *Journal of Geophysical Research*, *110*(1), B01303. https://doi.org/10.1029/2004jb003065

Ebinger, C. J., & Casey, M. (2001). Continental breakup in magmatic provinces: An Ethiopian example. *Geology*, *29*(6), 527–530. https://doi.org/10.1130/0091-7613(2001)029<0527:cbimpa>2.0.co;2

Ebinger, C. J., & Sleep, N. H. (1998). Cenozoic magmatism throughout east Africa resulting from impact of a single plume. *Nature*, *395*(6704), 788–791. https://doi.org/10.1038/27417

Efron, B., & Tibshirani, R. (1986). Bootstrap methods for standard errors, confidence intervals, and other measures of statistical accuracy. *Statistical Science*, *1*(1), 54–75. https://doi.org/10.1214/ss/1177013815

Fadel, I., Paulssen, H., van der Meijde, M., Kwadiba, M., Ntibinyane, O., Nyblade, A., & Durrheim, R. (2020). Crustal and upper mantle shear wave velocity structure of Botswana: The 3 April 2017 central Botswana earthquake linked to the East African Rift System. *Geophysical Research Letters*, *47*(4), e2019GL085598. https://doi.org/10.1029/2019gl085598

Fadel, I., van der Meijde, M., & Paulssen, H. (2018). Crustal structure and dynamics of Botswana. *Journal of Geophysical Research: Solid Earth*, *123*(12), 10659–10671. https://doi.org/10.1029/2018jb016190

Feng, M., Wei, S., Chen, L., Muksin, U., Lythgoe, K., Wang, T., & Wu, Z. (2023). Pervasive crustal volcanic mush in the highly stretched Sunda plate margin of Northern Sumatra. *Geophysical Research Letters*, *50*(21), e2023GL104391. https://doi.org/10.1029/2023gl104391

Foley, S. F., Yaxley, G. M., Rosenthal, A., Buhre, S., Kiseeva, E. S., Rapp, R. P., & Jacob, D. E. (2009). The composition of near-solidus melts of peridotite in the presence of CO_2 and H_2O between 40 and 60 kbar. *Lithos*, *112*, 274–283. https://doi.org/10.1016/j.lithos.2009.03.020

Furman, T. (2007). Geochemistry of East African rift basalts: An overview. *Journal of African Earth Sciences*, *48*(2–3), 147–160. https://doi.org/10.1016/j.jafrearsci.2006.06.009

Gao, S., Liu, K., Abdelsalam, M., & Hogan, J. (2012). Seismic Arrays for African Rift Initiation [Dataset]. *International Federation of Digital Seismograph Networks*. https://doi.org/10.7914/SN/XK_2012

George, R., Rogers, N. W., & Kelley, S. P. (1998). Earliest magmatism in Ethiopia: Evidence for two mantle plumes in one flood basalt province. *Geology*, *26*(10), 923–926. https://doi.org/10.1130/0091-7613(1998)026<0923:emieef>2.3.co;2

Grauch, V. J. S., Bauer, P. W., Drenth, B. J., & Kelson, K. I. (2017). A shifting rift-Geophysical insights into the evolution of Rio Grande rift margins and the Embudo transfer zone near Taos, New Mexico. *Geosphere*, *13*(3), 870–910. https://doi.org/10.1130/ges01425.1

Hammond, J. O. S., Kendall, J.-M., Stuart, G. W., Keir, D., Ebinger, C., Ayele, A., & Belachew, M. (2011). The nature of the crust beneath the Afar triple junction: Evidence from receiver functions. *Geochemistry, Geophysics, Geosystems*, *12*(12), 12004–12027. https://doi.org/10.1029/2011gc003738

Hansen, S. E., Nyblade, A. A., & Benoit, M. H. (2012). Mantle structure beneath Africa and Arabia from adaptively parameterized P-wave tomography: Implications for the origin of Cenozoic Afro-Arabian tectonism. *Earth and Planetary Science Letters*, *319–320*(48), 23–34. https://doi.org/10.1016/j.epsl.2011.12.023

Hodgson, I., Illsley-Kemp, F., Gallacher, R. J., Keir, D., Ebinger, C. J., & Mtelela, K. (2017). Crustal structure at a young continental rift: A receiver function study from the Tanganyika rift. *Tectonics*, *36*(12), 2806–2822. https://doi.org/10.1002/2017tc004477

Hopper, E., Gaherty, J. B., Shillington, D. J., Accardo, N. J., Nyblade, A. A., Holtzman, B. K., et al. (2020). Preferential localized thinning of lithospheric mantle in the melt-poor Malawi Rift. *Nature Geoscience*, *13*(8), 584–589. https://doi.org/10.1038/s41561-020-0609-y

Keen, C. E., Courtney, R. C., Dehler, S. A., & Williamson, M.-C. (1994). Decompression melting at rifted margins: Comparison of model predictions with the distribution of igneous rocks on the eastern Canadian margin. *Earth and Planetary Science Letters*, *121*(3–4), 403–416. https://doi.org/10.1016/0012-821x(94)90080-9

Keranen, K., Klemperer, S. L., Gloaguen, R., & EAGLE Working Group (2004). Three-dimensional seismic imaging of a protoridge axis in the Main Ethiopian rift. *Geology*, *32*(11), 949–952. https://doi.org/10.1130/g20737.1

Le Gall, B., Tshoso, G., Jourdan, F., Feraud, G., Bertrand, H., Tiercelin, J. J., et al. (2002). $^{40}Ar/^{39}Ar$ geochronology and structural data from the giant Okavango and related mafic dyke swarms, Karoo igneous province, northern Botswana. *Earth and Planetary Science Letters*, *202*(3–4), 595–606. https://doi.org/10.1016/s0012-821x(02)00763-x

Leseane, K., Atekwana, E. A., Mickus, K. L., Abdelsalam, M. G., Shemang, E. M., & Atekwana, E. A. (2015). Thermal perturbations beneath the incipient Okavango Rift Zone, northwest Botswana. *Journal of Geophysical Research: Solid Earth*, *120*(2), 1210–1228. https://doi.org/10.1002/2014jb011029

Levin, V., & Park, J. (1997). P-SH conversions in a flat-layered medium with anisotropy of arbitrary orientation. *Geophysical Journal International*, *131*(2), 253–266. https://doi.org/10.1111/j.1365-246x.1997.tb01220.x

Link, F., Rumpker, G., & Kaviani, A. (2020). Simultaneous inversion for crustal thickness and anisotropy by multiphase splitting analysis of receiver functions. *Geophysical Journal International*, *223*(3), 2009–2026. https://doi.org/10.1093/gji/ggaa435

Lithgow-Bertelloni, C., & Silver, P. G. (1998). Dynamic topography, plate driving forces and the African superswell. *Nature*, *395*(6699), 269–272. https://doi.org/10.1038/26212

Lombardi, D., Braunmiller, J., Kissling, E., & Giardini, D. (2008). Moho depth and Poisson's ratio in the Western-Central Alps from receiver functions. *Geophysical Journal International*, *173*(1), 249–264. https://doi.org/10.1111/j.1365-246x.2007.03706.x

Mayle, M., & Harry, D. L. (2023). Syn-rift magmatism and sequential melting of fertile lithologies in the lithosphere and asthenosphere. *Journal of Geophysical Research: Solid Earth*, *128*(9), e2023JB027072. https://doi.org/10.1029/2023jb027072

Moore, A. E., & Larkin, P. (2001). Drainage evolution in south-central Africa since the breakup of Gondwana. *South African Journal of Geology*, *104*(1), 47–68. https://doi.org/10.2113/104.1.47

Ni, S. D., Ding, X., Helmberger, D. V., & Gurnis, M. (1999). Low-velocity structure beneath Africa from forward modeling. *Earth and Planetary Science Letters*, *170*(4), 497–507. https://doi.org/10.1016/s0012-821x(99)00121-1

Nyblade, A. A., & Robinson, S. W. (1994). The African superswell. *Geophysical Research Letters*, *21*(9), 765–768. https://doi.org/10.1029/94gl00631

Ogden, C. S., Bastow, I. D., Gilligan, A., & Rondenay, S. (2019). A reappraisal of the H-κ stacking technique: Implications for global crustal structure. *Geophysical Journal International*, *219*(3), 1491–1513. https://doi.org/10.1093/gji/ggz364

Ortiz, K., Nyblade, A., van der Meijde, M., Paulssen, H., Kwadiba, M., Ntibinyane, O., et al. (2019). Upper mantle P- and S-wave velocity structure of the Kalahari Craton and surrounding Proterozoic terranes, southern Africa. *Geophysical Research Letters*, *46*(16), 9509–9518. https://doi.org/10.1029/2019gl084053

Penn State University. (2004). AfricaArray [Dataset]. *International Federation of Digital Seismograph Networks*. https://doi.org/10.7914/SN/AF

Plasman, M., Tiberi, C., Ebinger, C., Gautier, S., Albaric, J., Peyrat, S., et al. (2017). Lithospheric low-velocity zones associated with a magmatic segment of the Tanzania Rift, East Africa. *Geophysical Journal International*, *210*(1), 465–481. https://doi.org/10.1093/gji/ggx177

Pretorius, D. A. (1984). *The Kalahari Foreland, its marginal troughs and overthrust belts, and the regional structure of Botswana (Information circular 169)*. University of the Witwatersrand.

Reed, C. A., Almadani, S., Gao, S. S., Elsheikh, A. A., Cherie, S., Abdelsalam, M. G., et al. (2014). Receiver function constraints on crustal seismic velocities and partial melting beneath the Red Sea rift and adjacent regions, Afar Depression. *Journal of Geophysical Research: Solid Earth*, *119*(3), 2138–2152. https://doi.org/10.1002/2013jb010719

Reeves, C. (1972). Rifting in the Kalahari? *Nature*, *237*(5350), 95–96. https://doi.org/10.1038/237095a0

Ringrose, S., Huntsman-Mapila, P., Kampunzu, A. B., Downey, W., Coetzee, S., Vink, B., et al. (2005). Sedimentological and geochemical evidence for palaeo-environmental change in the Makgadikgadi subbasin, in relation to the MOZ rift depression, Botswana. *Palaeogeography, Palaeoclimatology, Palaeoecology*, *217*(3–4), 265–287. https://doi.org/10.1016/j.palaeo.2004.11.024

Ritsema, J., Ni, S., Helmberger, D. V., & Crotwell, H. P. (1998). Evidence for strong shear velocity reductions and velocity gradients in the lower mantle beneath Africa. *Geophysical Research Letters*, *25*(23), 4245–4248. https://doi.org/10.1029/1998gl900127

Roecker, S., Ebinger, C., Tiberi, C., Mulibo, G., Ferdinand-Wambura, R., Mtelela, K., et al. (2017). Subsurface images of the Eastern Rift, Africa, from the joint inversion of body waves, surface waves and gravity: Investigating the role of fluids in early-stage continental rifting. *Geophysical Journal International*, *210*(2), 931–950. https://doi.org/10.1093/gji/ggx220

Rooney, T. O. (2020). The Cenozoic magmatism of east Africa: Part V - magma sources and processes in the East African Rift. *Lithos*, *360–361*, 105296. https://doi.org/10.1016/j.lithos.2019.105296

Rychert, C. A., Hammond, J., Harmon, N., Kendall, J. M., Keir, D., Ebinger, C., et al. (2012). Volcanism in the Afar Rift sustained by decompression melting with minimal plume influence. *Nature Geoscience*, *5*(6), 406–409. https://doi.org/10.1038/ngeo1455

Sun, M., Gao, S. S., Liu, K. H., Mickus, K., Fu, X., & Yu, Y. (2021). Receiver function investigation of crustal structure in the Malawi and Luangwa Rift Zones and adjacent areas. *Gondwana Research*, *89*, 168–176. https://doi.org/10.1016/j.gr.2020.08.015

Takei, Y. (2002). Effect of pore geometry on Vp/Vs: From equilibrium geometry to crack. *Journal of Geophysical Research*, *107*(B2), ECV6-1–ECV6-12. https://doi.org/10.1029/2001jb000522

Thybo, H., & Nielsen, C. A. (2009). Magma-compensated crustal thinning in continental rift zones. *Nature*, *457*(7231), 873–876. https://doi.org/10.1038/nature07688

Tsekhmistrenko, M., Sigloch, K., Hosseini, K., & Barruol, G. (2021). A tree of Indo-African mantle plumes imaged by seismic tomography. *Nature Geoscience*, *14*(8), 612–619. https://doi.org/10.1038/s41561-021-00762-9

Utrecht University (UU Netherlands). (1983). Nars [Dataset]. *International Federation of Digital Seismograph Networks*. https://doi.org/10.7914/SN/NR

Wang, T., Gao, S. S., Yang, Q., Chen, L., & Liu, K. H. (2022). Lithospheric structure underneath the Archean Tanzania Craton and adjacent regions from a joint inversion of receiver functions and Rayleigh-wave phase velocity dispersion. *Seismological Research Letters*, *93*(3), 1753–1767. https://doi.org/10.1785/0220210296

Wang, T., Gao, S. S., Yang, Q., & Liu, K. H. (2021). Crustal structure beneath the Ethiopian Plateau and adjacent areas from receiver functions: Implications for partial melting and magmatic underplating. *Tectonophysics*, *809*(6), 228857. https://doi.org/10.1016/j.tecto.2021.228857

Watanabe, T. (1993). Effects of water and melt on seismic velocities and their application to characterization of seismic reflectors. *Geophysical Research Letters*, *20*(24), 2933–2936. https://doi.org/10.1029/93gl03170

Wedmore, L. N. J., Biggs, J., Floyd, M., Fagereng, A., Mdala, H., Chindandali, P., et al. (2021). Geodetic constraints on cratonic microplates and broad strain during rifting of thick southern African lithosphere. *Geophysical Research Letters*, *48*(17), e2021GL093785. https://doi.org/10.1029/2021gl093785

Wessel, P., Luis, J. F., Uieda, L., Scharroo, R., Wobbe, F., Smith, W. H. F., & Tian, D. (2019). The generic mapping tools version 6. *Geochemistry, Geophysics, Geosystems*, *20*(11), 5556–5564. https://doi.org/10.1029/2019gc008515

White, R., & McKenzie, D. (1989). Magmatism at rift zones: The generation of volcanic continental margins and flood basalts. *Journal of Geophysical Research*, *94*(B6), 7685–7729. https://doi.org/10.1029/jb094ib06p07685

White, R. S., Smith, L. K., Roberts, A. W., Christie, P. A. F., & Kusznir, N. J., & the rest of the iSIMM Team. (2008). Lower-crustal intrusion on the North Atlantic continental margin. *Nature*, *452*(7186), 460–464. https://doi.org/10.1038/nature06687

WoldeGabriel, G., Aronson, J., & Walter, R. C. (1990). Geology, geochronology, and rift basin development in the central sector of the Main Ethiopia Rift. *Geological Society of America Bulletin*, *102*(4), 439–458. https://doi.org/10.1130/0016-7606(1990)102<0439:ggarbd>2.3.co;2

Wolfenden, E., Ebinger, C., Yirgu, G., Renne, P. R., & Kelley, S. P. (2005). Evolution of a volcanic rifted margin: Southern Red Sea, Ethiopia. *Geological Society of America Bulletin*, *117*(7–8), 846–864. https://doi.org/10.1130/b25516.1

Wright, T. J., Ebinger, C., Biggs, J., Ayele, A., Yirgu, G., Keir, D., & Stork, A. (2006). Magma-maintained rift segmentation at continental rupture in the 2005 Afar dyking episode. *Nature*, *442*(7100), 291–294. https://doi.org/10.1038/nature04978

Xu, H., Luo, Y., Yang, Y., Shen, W., Yin, X., Chen, G., et al. (2020). Three-dimensional crustal structures of the Shanxi Rift constructed by Rayleigh wave dispersion curves and ellipticity: Implication for sedimentation, intraplate volcanism, and seismicity. *Journal of Geophysical Research: Solid Earth*, *125*(11), e2020JB020146. https://doi.org/10.1029/2020jb020146

Xu, X., & Ma, X. (1992). Geodynamics of the Shanxi Rift system, China. *Tectonophysics*, *208*(1–3), 325–340. https://doi.org/10.1016/0040-1951(92)90353-8

Yu, Y., Gao, S. S., Moidaki, M., Reed, C. A., & Liu, K. H. (2015). Seismic anisotropy beneath the incipient Okavango rift: Implications for rifting initiation. *Earth and Planetary Science Letters*, *430*, 1–8. https://doi.org/10.1016/j.epsl.2015.08.009

Yu, Y., Liu, K. H., Reed, C. A., Moidaki, M., Mickus, K., Atekwana, E. A., & Gao, S. S. (2015). A joint receiver function and gravity study of crustal structure beneath the incipient Okavango Rift, Botswana. *Geophysical Research Letters*, *42*(20), 8398–8405. https://doi.org/10.1002/2015gl065811

Yu, Y., Song, J., Liu, K. H., & Gao, S. S. (2015). Determining crustal structure beneath seismic stations overlying a low-velocity sedimentary layer using receiver functions. *Journal of Geophysical Research: Solid Earth*, *120*(5), 3208–3218. https://doi.org/10.1002/2014jb011610

Zhu, L., & Kanamori, H. (2000). Moho depth variation in southern California from teleseismic receiver functions. *Journal of Geophysical Research*, *105*(B2), 2969–2980. https://doi.org/10.1029/1999jb900322

References From the Supporting Information

Berglund, H. T., Sheehan, A. F., Murray, M. H., Roy, M., Lowry, A. R., Nerem, R. S., & Blume, F. (2012). Distributed deformation across the Rio Grande Rift, great plains, and Colorado plateau. *Geology*, *40*(1), 23–26. https://doi.org/10.1130/g32418.1

Chen, L. (2014). Stretching factor estimation for the long-duration and multi-stage continental extensional tectonics: Application to the Baiyun Sag in the northern margin of the South China Sea. *Tectonophysics*, *611*, 167–180. https://doi.org/10.1016/j.tecto.2013.11.026

Chen, Y., Chen, J., Li, S., Yu, Z., Liu, X., & Shen, X. (2021). Variations of crustal thickness and average Vp/Vs ratio beneath the Shanxi Rift, North China, from receiver functions. *Earth Planets and Space*, *73*(1), 200. https://doi.org/10.1186/s40623-021-01528-8

Cunningham, E., & Lekic, V. (2019). Constraining crustal structure in the presence of sediment: A multiple converted wave approach. *Geophysical Journal International*, *219*(1), 313–327. https://doi.org/10.1093/gji/ggz298

Delph, J. R., & Porter, R. C. (2015). Crustal structure beneath southern Africa: Insight into how tectonic events affect the Mohorovicic discontinuity. *Geophysical Journal International*, *200*(1), 254–264. https://doi.org/10.1093/gji/ggu376

Durrheim, R. J., & Green, R. W. E. (1992). A seismic refraction investigation of the Archaean Kaapvaal Craton, South Africa, using mine tremors as the energy source. *Geophysical Journal International*, *108*(3), 812–832. https://doi.org/10.1111/j.1365-246x.1992.tb03472.x

Gao, S. S., Liu, K. H., & Chen, C. (2004). Significant crustal thinning beneath the Baikal rift zone: New constraints from receiver function analysis. *Geophysical Research Letters*, *31*(20), L20610. https://doi.org/10.1029/2004gl020813

Gore, J., James, D. E., Zengeni, T. G., & Gwavava, O. (2009). Crustal structure of the Zimbabwe craton and the Limpopo belt of southern Africa: New constraints from seismic data and implications for its evolution. *South African Journal of Geology*, *112*(3–4), 213–228. https://doi.org/10.2113/gssajg.112.3-4.213

Ito, H., DeVilbiss, J., & Nur, A. (1979). Compressional and shear waves in saturated rock during water-steam transition. *Journal of Geophysical Research*, *84*(B9), 4731–4735. https://doi.org/10.1029/jb084ib09p04731

Julian, B. R., Pitt, A. M., & Foulger, G. R. (1998). Seismic image of a CO_2 reservoir beneath a seismically active volcano. *Geophysical Journal International*, *133*(1), F7–F10. https://doi.org/10.1046/j.1365-246x.1998.1331540.x

Kinabo, B. D., Hogan, J. P., Atekwana, E. A., Abdelsalam, M. G., & Modisi, M. P. (2008). Fault growth and propagation during incipient continental rifting: Insights from a combined aeromagnetic and Shuttle Topography Mission digital elevation model investigation of the Okavango Rift Zone, northwest Botswana. *Tectonics*, *27*(3), 1–16. https://doi.org/10.1029/2007tc002154

Kong, F., Gao, S. S., Liu, K. H., Ding, W., & Li, J. (2020). Slab dehydration and mantle upwelling in the vicinity of the Sumatra subduction zone: Evidence from receiver function imaging of mantle transition zone discontinuities. *Journal of Geophysical Research: Solid Earth*, *125*(9), e2020JB019381. https://doi.org/10.1029/2020jb019381

Krylov, S. V., Mandelbaum, M. M., Mishen'kin, B. P., Mishen'kina, Z. P., Petric, G. V., & Seleznev, V. C. (1981). *The interior of Baikal from seismic data*. Nauka. (in Russian).

Langston, C. A. (2011). Wave-field continuation and decomposition for passive seismic imaging under deep unconsolidated sediments. *Bulletin of the Seismological Society of America*, *101*(5), 2176–2190. https://doi.org/10.1785/0120100299

Liu, K. H., & Gao, S. S. (2010). Spatial variations of crustal characteristics beneath the Hoggar swell, Algeria, revealed by systematic analyses of receiver functions from a single seismic station. *Geochemistry, Geophysics, Geosystems*, *11*(8), Q08011. https://doi.org/10.1029/2010gc003091

Logatchev, N. A., Zorin, Y. A., & Rogozhina, V. A. (1983). Baikal rift: Active or passive? Comparison of the Baikal and Kenya rift zones. *Tectonophysics*, *94*(1–4), 223–240. https://doi.org/10.1016/0040-1951(83)90018-5

Mavko, G., & Mukerji, T. (1995). Seismic pore space compressibility and Gassmann's relation. *Geophysics*, *60*(6), 1743–1749. https://doi.org/10.1190/1.1443907

McKenzie, D. (1978). Some remarks on the development of sedimentary basins. *Earth and Planetary Science Letters*, *40*(1), 25–32. https://doi.org/10.1016/0012-821x(78)90071-7

McKenzie, D. P., Davies, D., & Molnar, P. (1970). Plate tectonics of the Red Sea and east Africa. *Nature*, *226*(5242), 243–248. https://doi.org/10.1038/226243a0

Modisi, M. P., Atekwana, E. A., Kampunzu, A. B., & Ngwisanyi, T. H. (2000). Rift kinematics during the incipient stages of continental extension: Evidence from the nascent Okavango rift basin, northwest Botswana. *Geology*, *28*(10), 939–942. https://doi.org/10.1130/0091-7613(2000)28<939:rkdtis>2.0.co;2

Morgan, P., Seager, W. R., & Golombek, M. P. (1986). Cenozoic thermal, mechanical and tectonic evolution of the Rio Grande Rift. *Journal of Geophysical Research*, *91*(B6), 6263–6276. https://doi.org/10.1029/jb091ib06p06263

Nair, S. K., Gao, S. S., Liu, K. H., & Silver, P. G. (2006). Southern African crustal evolution and composition: Constraints from receiver function studies. *Journal of Geophysical Research*, *111*(2), B02304. https://doi.org/10.1029/2005jb003802

Nguuri, T. K., Gore, J., James, D. E., Webb, S. J., Wright, C., Zengeni, T. G., et al. (2001). Crustal structure beneath southern Africa and its implications for the formation and evolution of the Kaapvaal and Zimbabwe cratons. *Geophysical Research Letters*, *28*(13), 2501–2504. https://doi.org/10.1029/2000gl012587

10.1029/2024GL111814

Pouclet, A., Bellon, H., & Bram, K. (2016). The Cenozoic volcanism in the Kivu rift: Assessment of the tectonic setting, geochemistry, and geochronology of the volcanic activity in the South-Kivu and Virunga regions. *Journal of African Earth Sciences*, *121*, 219–246. https://doi.org/10.1016/j.jafrearsci.2016.05.026

Press, W. H., Teukolsky, S. A., Vetterling, W. T., & Flannery, B. P. (1992). *Numerical recipes in FORTRAN* (2nd ed.). Cambridge Univ. Press.

Scholz, C. H., Koczynski, T. A., & Hutchins, D. G. (1976). Evidence for incipient rifting in southern Africa. *Geophysical Journal International*, *44*(1), 135–144. https://doi.org/10.1111/j.1365-246x.1976.tb00278.x

Schulte-Pelkum, V., & Mahan, K. H. (2014). A method for mapping crustal deformation and anisotropy with receiver functions and first results from USArray. *Earth and Planetary Science Letters*, *402*, 221–233. https://doi.org/10.1016/j.epsl.2014.01.050

Stuart, G. W., Bastow, I. D., & Ebinger, C. J. (2006). Crustal structure of the northern Main Ethiopian Rift from receiver function studies. *Geological Society, London, Special Publications*, *259*(1), 253–267. https://doi.org/10.1144/gsl.sp.2006.259.01.20

Su, P., He, H., Tan, X., Liu, Y., Shi, F., & Kirby, E. (2021). Initiation and evolution of the Shanxi Rift System in North China: Evidence from low-temperature thermochronology in a plate reconstruction framework. *Tectonics*, *40*(3), e2020TC006298. https://doi.org/10.1029/2020tc006298

ten Brink, U. S., & Taylor, M. H. (2002). Crustal structure of central Lake Baikal: Insights into intracontinental rifting. *Journal of Geophysical Research*, *107*(B7), 2132. https://doi.org/10.1029/2001jb000300

Wang, Q., Niu, F., Gao, Y., & Chen, Y. (2016). Crustal structure and deformation beneath the NE margin of the Tibetan plateau constrained by teleseismic receiver function data. *Geophysical Journal International*, *204*(1), 167–179. https://doi.org/10.1093/gji/ggv420

Wilson, D., Aster, R., Ni, J., Grand, S., West, M., Gao, W., et al. (2005). Imaging the seismic structure of the crust and upper mantle beneath the Great Plains, Rio Grande Rift, and Colorado Plateau using receiver functions. *Journal of Geophysical Research*, *110*(B5), B05306. https://doi.org/10.1029/2004jb003492

Wright, J. A., & Hall, J. (1990). Deep seismic profiling in the Nosop basin, Botswana: Cratons, mobile belts and sedimentary basins. *Tectonophysics*, *173*(1–4), 333–343. https://doi.org/10.1016/0040-1951(90)90228-z

Youssof, M., Thybo, H., Artemieva, I. M., & Levander, A. (2013). Moho depth and crustal composition in Southern Africa. *Tectonophysics*, *609*(1), 267–287. https://doi.org/10.1016/j.tecto.2013.09.001

Zelt, B. C., & Ellis, R. M. (1999). Receiver-function studies in the Trans-Hudson orogen, Saskatchewan. *Canadian Journal of Earth Sciences*, *36*(4), 585–603. https://doi.org/10.1139/cjes-36-4-585

Zhou, Z., Thybo, H., Tang, C.-C., Artemieva, I., & Kusky, T. (2023). Test of P-wave receiver functions for a seismic velocity and gravity model across the Baikal Rift Zone. *Geophysical Journal International*, *232*(1), 176–189. https://doi.org/10.1093/gji/ggac335